Thermodynamic stabilities of ternary metal borides: An *ab initio* guide for synthesizing layered superconductors

Aleksey N. Kolmogorov,[1] Matteo Calandra,[2] and Stefano Curtarolo[3]

[1]*Department of Materials, University of Oxford, Parks Road, Oxford OX1 3PH, United Kingdom*
[2]*Institut de Mineralogie et de Physique des Milieux Condensés, case 115, 4 place Jussieu, 75252 Paris Cedex 05, France*
[3]*Department of Mechanical Engineering and Materials Science, Duke University, Durham, North Carolina 27708, USA*

Density-functional theory calculations have been used to identify stable layered Li-M-B crystal structure phases derived from a recently proposed binary metal-sandwich (MS) lithium monoboride superconductor. We show that the MS lithium monoboride gains in stability when alloyed with electron-rich metal diborides; the resulting ordered $Li_{2(1-x)}M_xB_2$ ternary phases may form under normal synthesis conditions in a wide concentration range of x for a number of group-III-V metals M. In an effort to preselect compounds with the strongest electron-phonon coupling we examine the softening of the in-plane boron phonon mode at Γ in a large class of metal borides. Our results reveal interesting general trends for the frequency of the in-plane boron phonon modes as a function of the boron-boron bond length and the valence of the metal. One of the candidates with a promise to be an MgB_2-type superconductor, Li_2AlB_4, has been examined in more detail: According to our *ab initio* calculations of the phonon dispersion and the electron-phonon coupling λ, the compound should have a critical temperature of $\sim$4 K.

PACS number(s): 74.70.Ad, 74.70.Dd, 63.20.K−

I. INTRODUCTION

Observation and explanation of the superconducting transition in MgB_2 at an unexpectedly high temperature of 39 K (Refs. [1] and [2]) have stimulated extensive research aimed at developing related layered phonon-mediated superconductors.[3–13] Interesting results have been recently obtained for carbon-based layered materials: The efforts to adjust the properties of graphite via intercalation with various metals have led to the discovery of a CaC_6 superconductor with a critical temperature of 11.5 K (Refs. [9] and [10]) (15.1 K under hydrostatic pressure[11]).

Tuning the properties of boron-based superconductors has proven to be difficult because, despite the existence of over a dozen of stable metal diborides with the C32 structure,[14–16] only one of them, MgB_2, has the hole-doped boron $p\sigma$ states that couple strongly to the in-plane boron phonon modes.[2] For comparison, critical temperatures in other C32-MB_2 superconductors, such as TaB_2 or NbB_2,[4–6] do not exceed 10 K because these electron-rich compounds have fully occupied boron $p\sigma$ bands and thus lack the important nearly two-dimensional Fermi surfaces. The attempts to raise T_c in MgB_2 via substitutional doping have been unsuccessful for various reasons: i) Electron doping led to the decrease in the electron-phonon coupling due mainly to the filling of the $p\sigma$ band;[2] ii) hole doping or substitution of Mg with large metals turned out to be thermodynamically unfavorable;[17,18] and iii) codoping of MgB_2 with Li-Al Li-C caused the reduction in the T_c because of the concurrent filling of the $p\sigma$ band and depletion of the $p\pi$ band.[19] Recently, Palnichenko *et al.* have reported interesting results on a possible onset of superconductivity in MgB_2 after thermal treatment in the presence of Rb, Cs, and Ba; the structure of the resultant materials and the mechanism of the T_c enhancement have yet to be determined.[20,21]

Identification and synthesis of new stable compounds will be a critical step to overcome the limitations of the existing layered metal borides and to have a chance of obtaining better superconductors. Using a data-mining approach we have recently found a previously unknown metal-sandwich (MS) crystal structure and demonstrated that lithium monoboride in this configuration is marginally stable under ambient conditions and is likely to form under pressure.[12,22] Remarkably, our calculations indicated that, relative to MgB_2, MS-LiB has a higher density of boron $p\sigma$ states at the Fermi level,[12,22] a feature long sought for in MgB_2-related materials. Subsequent theoretical studies of the electron-phonon coupling predicted that the T_c in MS-LiB would be around 10 K.[23,24] The relatively low value of T_c has been attributed to an accidental electronic structure feature present in the pristine MS-LiB: The crossing of the $p\pi$ bands happens to be exactly at the Fermi level.[23,24] After examining the compound's response to hydrostatic pressure and substitutional doping we have concluded that the recovery of the $p\pi$ density of states (DOS) at the Fermi level would be accompanied by an unfortunate drop of the $p\sigma$ DOS under these conditions.[24] The question of whether it could be possible to tune the properties of MS-LiB to obtain higher T_c remains open.

In this work we expand the search for stable crystal structure phases to ternary metal borides. Namely, we use density-functional theory calculations to explore the relative stability of different layered configurations with composition $Li_{2(1-x)}M_xB_2$ for a library of over 30 metals M. We show that MS lithium monoboride gains in stability when alloyed with electron-rich metal diborides; the resulting ordered $Li_{2(1-x)}M_xB_2$ ternary phases may form under normal synthesis conditions in a large concentration range of x for a number of group-III-V metals M. For several promising candidates we evaluate the softening of the in-plane boron phonon mode at Γ in order to identify which of these compounds has large coupling to the in-plane boron modes (similarly to what happens in MgB_2). For one case, Li_2AlB_4, we also perform a

full calculation of the critical temperature. We believe that our results will be of considerable help to experimental groups working on the development of new boron-based layered superconductors.

The paper is organized as follows: In Sec. II we describe the geometry of the ternary MS structures. Section III is devoted to the zero-temperature thermodynamic stability of $Li_{2(1-x)}M_xB_2$ phases and to the special case $Li_{2(1-x)}Al_xB_2$. Electronic properties of two representatives, Li_2AlB_4 and Li_2TiB_4, are addressed in Sec. IV. In Sec. V we examine the phonon softening in a large set of metal borides. In Sec. VI we present the *ab initio* superconductivity analysis of Li_2AlB_4. Conclusions are given in Sec. VII.

II. $Li_{2(1-x)}M_xB_2$ METAL-SANDWICH STRUCTURES

Consideration of ternary Li-*M*-B systems dramatically increases the number of candidates to be screened because one should check both different compositions and various populations of metal sites. We reduce the search space by recalling the binding trends for the binary MS metal borides demonstrated in our previous study.[22] Namely, the MS lithium monoboride has plenty of available bonding boron $p\sigma$ states and may additionally stabilize when mixed with electron-rich metals. Because straightforward substitutional doping generally causes strain and loss of binding within the metal layers[18,25] we separate regions with different metal species by boron layers and, thus, avoid putting different metals in direct contact. This idea follows a natural segregation tendency in layered borides, which has been observed, for instance, in MgB_2 under heavy Al doping: The resulting compound was a C32 superstructure with alternating Mg and Al layers.[26]

Our candidate segregated superstructures are built by combining MS-LiB and C32-MB_2 unit cells. Since there are numerous possibilities to stack metal and boron layers, it is convenient to adopt the following compact notation: MS1-LiB and C32-MB_2 basic units will be denoted as "1"- and "0"-unit, respectively. In this way one can uniquely specify the structure with a string of ones and zeros. Note that the presence of one "1"-unit results in a stacking shift along the *c* axis which makes the unit cell rhombohedral.[12,22] For convenience, in candidate phases containing an even number of "1"-units we choose to reflect every second "1"-unit in the (x,y) plane to obtain a hexagonal unit cell. This choice is expected to not affect our results, since we have found no appreciable differences in the properties of the rhombohedral and hexagonal allotropes of MS-LiB.[12] Examples of two superstructures with small unit cells are 10-Li_2MB_4 [Fig. 1(c)] and 110-Li_4MB_6 [Fig. 1(b)], the latter being the superposition of MS2-LiB and C32-MB_2.

Figure 1 shows that such compounds are located along the red line on the ternary phase diagram. Note that MS-LiB is marginally stable (the known competing phase LiB_y has a completely different structure[22]). This implies that if (i) the C32-MB_2 exists and (ii) the relative stability of the MS ternary phases along this line is negative, then one would have a better chance of synthesizing the MS ternary compounds from elemental materials rather than the two binaries MS2-
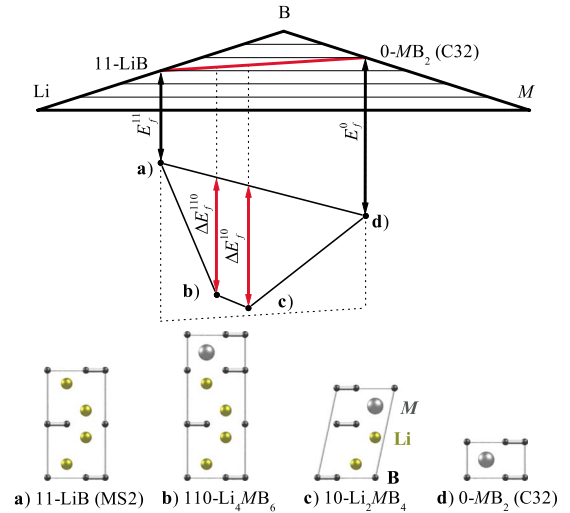

FIG. 1. (Color online) Structure of the proposed ternary metal-sandwich phases and their location on a schematic ternary (Li-*M*-B) phase diagram. Formation energies are shown along the vertical axis. The relative stability is calculated with respect to 11-LiB (MS2) and 0-MB_2 (C32) (notation explained in the text).

LiB and MB_2 separately. Of course, one needs to make sure that no other competing phase forms, which can be a challenging task for ternary systems.

III. THERMODYNAMIC STABILITY

A. Computational details

In the evaluation of the low temperature stability of ternary compounds, we rely on the "*ab initio* formation energy" criterion, which has been shown to be a reliable approach for binary systems[27,28] [expected probability of predicting the correct experimental compounds or immiscibilities is $\eta^* \approx 97.3\%$ as defined in Eq. (5) of Ref. 29]. *Ab initio* total-energy calculations are performed in the generalized gradient approximation with projector augmented wave (PAW) (Ref. 30) pseudopotentials and Perdew, Burke, and Ernzerhof[31] exchange-correlation functional, as implemented in VASP.[32,33] Because of a significant charge transfer between metal and boron in most structures considered we use PAW pseudopotentials in which semicore states are treated as valence. This is especially important for the Li-B system as discussed in Refs. 34 and 12. Simulations are carried out at zero temperature and without zero-point motion; spin polarization is used only for borides of Fe, Co, and Ni. We use an energy cutoff of 398 eV and at least 4000/(number of atoms in unit cell) **k** points distributed on a Monkhorst-Pack mesh.[35] All structures are fully relaxed and numerically converged to within 1–2 meV/atom.

B. Stability of Li_2MB_4 phases

Figure 2 shows the relative formation energy ΔE_f^{10} of 10-Li_2MB_4 metal borides [Fig. 1(c)] with respect to phase separation into 11-LiB (MS2) and 0-MB_2 (C32):
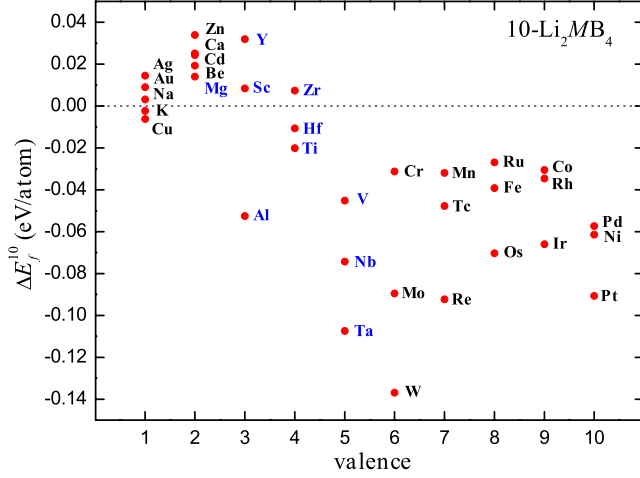
FIG. 2. (Color online) Relative stability of the 10-Li_2MB_4 metal borides [Fig. 1(c)] with respect to phase separation into 11-LiB (MS2) and 0-MB_2 (C32) [see Eq. (1)] as a function of metal valence. The group-II-V metals highlighted in blue form stable C32-type diborides.

$$\Delta E_f^{10} \equiv E_f^{10} - \frac{4}{7}E_f^{11} - \frac{3}{7}E_f^0 \qquad (1)$$

(all formation energies are per atom). We observe that there are many metals that can stabilize MS2-LiB and a number of them do have stable C32-MB_2 phases (M=Al, Hf, Ti, V, Nb, Ta).[15,36] Considering that metals M=Hf, Ti, V, Nb, Ta have no reported stable compounds with Li or Li-B,[14,15] there is a good chance that the predicted layered phases will form in the Li-M-B (M=V, Nb, Ta) ternary systems. Note that stable structures for several transition-metal diborides have larger unit cells with buckled boron layers and different location of metal sites [WB$_2$ ($hP12$, $hR18$), MoB$_2$ ($hR18$), RuB$_2$ and

OsB$_2$ ($oP6$) (the δ phase[37] is basically a noncorrugated $oP6$)]. For example, the oP6-RuB$_2$ phase is favored over C32-RuB$_2$ by about 0.4 eV/atom, which would make 10-Li$_2$RuB$_4$ unstable. However, one could expand the library of possible ternary configurations by creating more stable MS sequences with buckled boron layers. As for the mono- and divalent metal diborides, it is not surprising that they cannot improve the stability of MS-LiB in the corresponding ternary alloy because they are underdoped themselves.[16] Structural and electronic properties for selected proposed 1010-Li$_2MB_4$ phases are summarized in Table I.

C. Li-Al-B system

Aluminum is a special case because it is the least electron-rich metal on the list that provides the desired stabilization for the ternary MS configurations. The sizeable 50-meV/atom energy gain for 10-Li$_2$AlB$_4$ indicates that this compound would be stable with respect to C32-AlB$_2$ and the known off-stoichiometry LiB$_y$ as well.[22] For the analysis of the thermodynamic stability of Li$_{2(x-1)}$Al$_x$B$_2$ we also need to consider the known stable Li-Al binary phases B32-LiAl, hR15-Li$_3$Al$_2$, and mS26-Li$_9$Al$_4$ (Refs. 15, 38, and 39) and the only reported ternary LiAlB$_{14}$ compound,[40] which was observed in experiments on doping AlB$_2$ with Li.[41]

The location of these phases on the Li-Al-B phase diagram is shown in Fig. 3. Because 10-Li$_2$AlB$_4$ lies very close to the line connecting LiAlB$_{14}$ and mS26-Li$_9$Al$_4$, its relative stability will be defined primarily by the formation energies of these two compounds. We find that 10-Li$_2$AlB$_4$ is virtually degenerate in energy with respect to the mixture of LiAlB$_{14}$, mS26-Li$_9$Al$_4$, and Li at zero temperature and pressure and without zero-point corrections; the finite-temperature contributions must have a negative effect on the 10-Li$_2$AlB$_4$ relative stability, as there are no reports on the formation of this compound.

TABLE I. Structural and electronic properties of the proposed 1010-Li$_2MB_4$ phases for metals M that have stable C32-MB_2 phases. We list fully relaxed lattice vectors and Wyckoff positions for the $P6_3/mmc$ (no. 194) unit cells: B1 ($4f$) $(1/3,2/3,z_{B1})$; B2 ($4e$) $(0,0,z_{B2})$; Li ($4f$) $(1/3,2/3,z_{Li})$; and M ($2c$) $(1/3,2/3,1/4)$. $E_\Gamma^{\sigma,1}$ and $E_\Gamma^{\sigma,2}$ and positions of the boron σ states above the Fermi level at the Γ point and ΔE_f^{1010} is a relative formation energy per atom with respect to MS2-LiB and C32-MB_2. ΔE_f^{1010} can be obtained from Eq. (1) by replacing E_f^{10} with E_f^{1010} since the two phases have the same composition. Band structures for 1010-Li$_2$AlB$_4$ and 1010-Li$_2$TiB$_4$ are shown in Figs. 5 and 6, respectively.

| M in 1010-Li$_2MB_4$	a (Å)	c (Å)	z_{B1}	z_{B2}	z_{Li}	$E_\Gamma^{\sigma,1}$ (eV)	$E_\Gamma^{\sigma,2}$ (eV)	ΔE_f^{1010} (eV/atom)
Mg	3.048	18.94	0.6560	0.6560	0.4214	0.93	0.75	0.014
Al	3.012	18.46	0.6643	0.6644	0.4198	0.62	0.14	−0.052
Sc	3.116	17.77	0.6524	0.6526	0.4263	0.78	−0.21	0.009
Y	3.225	16.14	0.6298	0.6302	0.4482	0.55	−0.13	0.033
Ti	3.040	17.99	0.6626	0.6627	0.4197	0.28	−1.54	−0.019
Zr	3.138	17.85	0.6514	0.6515	0.4265	0.16	−1.25	0.008
Hf	3.119	18.20	0.6558	0.6559	0.4229	0.05	−1.40	−0.010
V	2.968	18.48	0.6670	0.6670	0.4181	−0.04	−2.43	−0.044
Nb	3.044	19.17	0.6610	0.6610	0.4188	−0.28	−2.45	−0.074
Ta	3.036	19.12	0.6615	0.6615	0.4194	−0.48	−2.61	−0.108
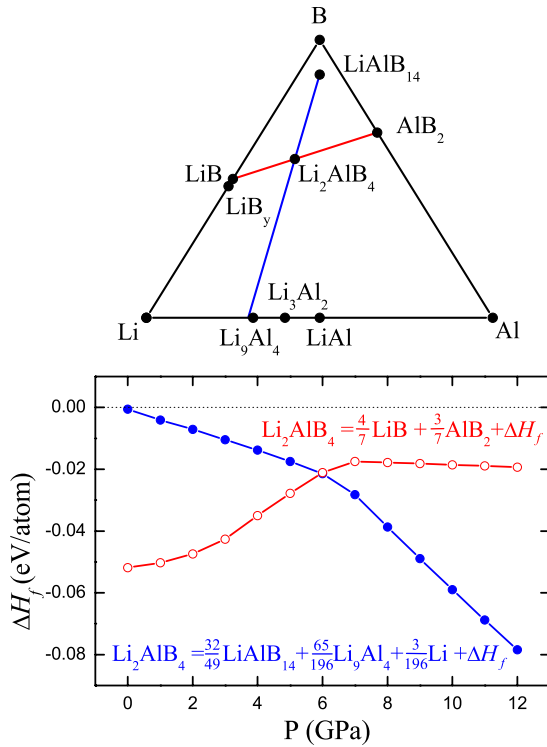
FIG. 3. (Color online) Top: location of known and predicted phases on the Li-Al-B phase diagram (the boron-rich Li-B and Al-B phases are not shown). Bottom: Relative stability of the proposed Li_2AlB_4 with respect to the decomposition along the lines shown on the top panel.

FIG. 4. Relative stability of $Li_{2(1-x)}Al_xB_2$ ternary metal borides with respect to the phase separation into 11-LiB (MS2) and 0-AlB_2 (C32). The dotted lines connect members of the $110\cdots0$ and $11110\cdots0$ series.

In order to stabilize the proposed phase one could use high pressures: As we have demonstrated previously the MS phases are unusually soft.[12,22] Indeed, the calculated relative formation enthalpy as a function of pressure for 10-Li_2AlB_4 in Fig. 3 either becomes negative (with respect to $LiAlB_{14}$, mS26-Li_9Al_4, and Li) or remains negative (with respect to 11-LiB and 0-AlB_2). The considerable change in slope at about 6 GPa is related to a sudden ~10% decrease in the 10-Li_2AlB_4 atomic volume at that pressure (Fig. 3). Overall, 10-Li_2AlB_4 compresses by over 25% when the pressure is increased from 0 GPa ($v = 10.4$ Å^3/atom, $H_f = -0.163$ eV/atom) to 12 GPa ($v = 7.7$ Å^3/atom, $H_f = -0.302$ eV/atom). For comparison, the $LiAlB_{14}$ phase is much more compact at $P = 0$ GPa ($v = 7.7$ Å^3/atom, $H_f = -0.168$ eV/atom) but compresses by only 5% at $P = 12$ GPa ($v = 7.3$ Å^3/atom, $H_f = -0.217$ eV/atom). These results suggest that this ternary and other binary boron-rich Li-B and Al-B phases,[15,42] also comprised of rigid boron polyhedra (e.g., Li_3B_{14}), should not prohibit the formation of the predicted layered compounds under the pressures considered.

There is strong evidence that another stable phase has formed in different experiments involving Li, Al, and B.[41,43] Monni *et al.*[43] suggested that their unidentified low-angle spurious peaks could belong to a binary Li-B phase. The authors purposely prepared a sample at the LiB_2 composition and indeed observed a matching set of the low-angle reflections (see Fig. 7 in Ref. 43). Their conclusion that the unknown phase is a binary Li-B compound agrees well with the observation of 12.2° and 20.9° peaks at 40%–50% Li com-
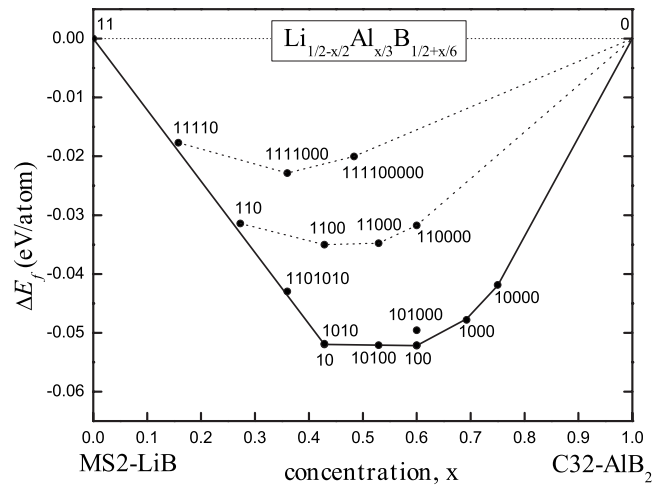
positions by Wang *et al.*[44] in 1978. However, in a series of detailed studies of the Li-B system Wörle *et al.*[45] have conclusively determined that such low-angle peaks correspond to $Li_6B_{18}(Li_2O)_x$ phases ($0 < x < 1$). The authors' latest analysis of the x-ray patterns and electron density distributions has indicated that the zeolitelike structure of $Li_6B_{18}(Li_2O)_x$ consists of interconnected boron octahedra with large tunnels filled with neutral Li_2O template.[45] Therefore, it appears that the stable oxygen-containing phase also formed in the earlier experiments involving Li and B at about 1:2 composition. This knowledge is important for future experiments on the ternary metal borides: In order to obtain the predicted layered compounds (whose stability can be affected by a few meV/atom) one needs to reduce the amount of oxygen in the system.

In order to determine whether there are more stable ternary MS configurations we calculate a number of Li-Al-B phases with various stacking sequences and compare their relative stability, ΔE_f, with respect to the phase separation in 11-LiB and 0-MB_2. The results in Fig. 4 suggest that 10-Li_2AlB_4 would be the most LiB-rich phase to form, while one could observe several AlB_2-rich phases at different concentrations (a similar phase diagram is obtained for the Li-Ti-B system). The effect of permutation of the "1" and "0" units on the energy at given composition is illustrated with the $10\cdots0$, $110\cdots0$, $11110\cdots0$ series shown in Fig. 4. These results clearly demonstrate the benefit of having stackings with alternating electron-poor "1"- and electron-rich "0"-units. For instance, 1010 is 20 meV/atom below 1100, which implies that the boron layer in the 11 block of 1100, surrounded by two Li layers on each side, does not take full advantage of the available charge provided by Al. This behavior is consistent with our previous observation that substitutional doping leads to the filling of boron states only in the layer closest to the dopant.[24]

Note that the boundary of the convex hull MS2-LiB$\leftrightarrow$C32-AlB_2 is determined by the $10\cdots0$ series, which implies that there is a thermodynamic driving force
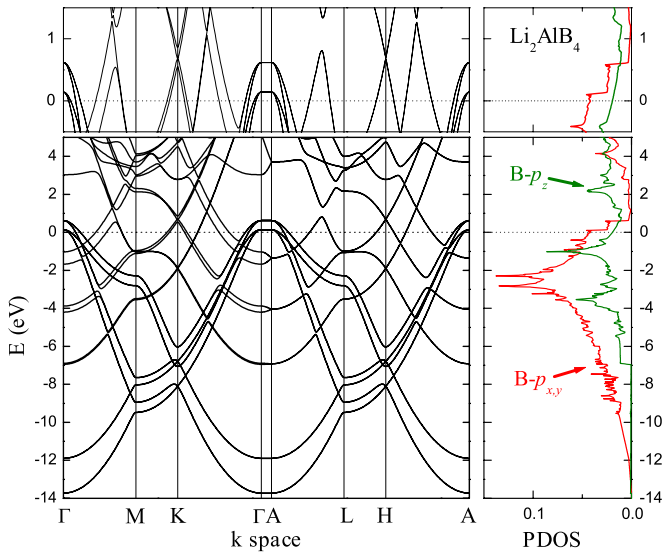
FIG. 5. (Color online). Band structure and partial density of states (PDOS) in 1010-Li_2AlB_4. The top panels show the region near the Fermi level (0 eV).
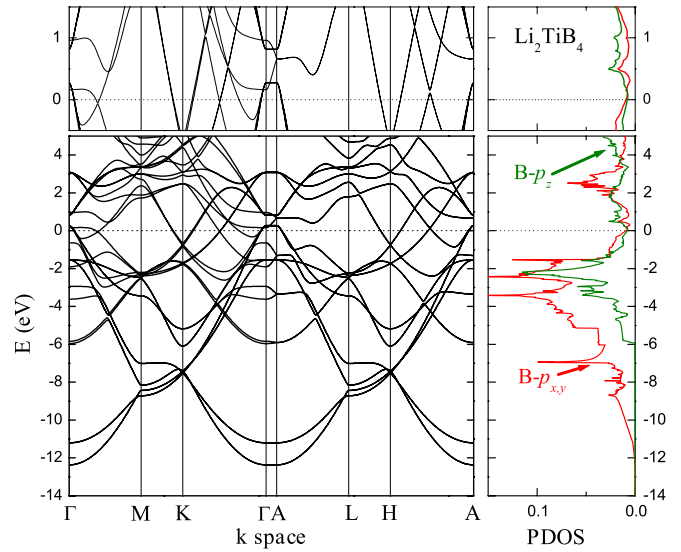

FIG. 6. (Color online). Band structure and partial density of states (PDOS) in 1010-Li_2TiB_4. The top panels show the region near the Fermi level (0 eV).

for the formation of "1"-units in the "0" matrix. Indeed, doing extrapolation over the $10\cdots0$ series we find that replacement of one Al layer via $nAlB_2+2Li=Li_2Al_{n-1}B_{2n}+Al$ is an exothermic reaction with $\Delta E=0.6$ eV/(Li atom) $(n\rightarrow\infty)$. There is an alternative exothermic reaction with an even bigger $\Delta E=0.8$ eV/(Li atom) $(n\rightarrow\infty)$ that preserves the C32 structure: $nAlB_2+Li=LiAl_{n-1}B_{2n}+Al$. Therefore, one would expect to see substitution of Al layers with Li first, and only at high Li concentration should the "1"-units start forming: In the limiting case of 1:1 Li:Al composition the reaction $LiAlB_4+Li=Li_2AlB_4$ would be energetically favorable by $\Delta E=0.4$ eV/(Li atom). However, these reactions have apparently not been observed due to the formation of the stable ternary $LiAlB_{14}$ and the oxygen-containing phases.[43]

In summary, based on our formation enthalpy calculations, Li_2AlB_4 is marginally stable with respect to the considered known compounds under normal conditions but can be stabilized by hydrostatic pressure. Considering the stabilizing effect of Al we expect a lower pressure threshold for the formation of the ternary MS-Li-Al-B phases compared to the case of the binary MS-Li-B phases.

More detailed studies should be carried out in the future to account for the finite-temperature contributions in the Gibbs free energy; this will be a difficult task because the boron-rich metal borides have large unit cells with fractional occupancies. In addition, one should consider not only compounds reported for a given ternary system, but also crystal structure phases observed in similar systems. For example, the absence of any stable Li-M-B phases (M=V, Nb, and Ta) in the ICSD database[14] could simply be an indication that these ternary systems have not been fully explored experimentally yet. It would not be surprising then if attempts to synthesize the predicted layered phases would lead to the formation of phases not considered here, such as the metal-rich Li_2Pd_3B superconductor comprised of linear chains of boron.[46] High-throughput simulation of selected ternary systems identified in our present work is a subject of future studies.

IV. ELECTRONIC PROPERTIES

It is interesting to see what changes in properties the combination of the nonsuperconducting MB_2 and potentially superconducting MS-LiB structures would induce. Electronic properties of the proposed MS ternary phases are examined for two representative 1010-Li_2AlB_4 and 1010-Li_2TiB_4 compounds with hexagonal unit cells (1010 and 10 phases are nearly degenerate in energy). Boron layers in the 1010 structure are indistinguishable, but there are two different sets of degenerate boron states derived from those in the original "0" and "1" metal borides. For example, in MS2-LiB the practically dispersionless $p\sigma$ states of boron are 1.0 eV above the Fermi level[12,22] while in C32-AlB_2 they are completely filled [$E_\Gamma^\sigma=-1.6$ eV, $E_A^\sigma=-1.0$ eV]; in 1010-Li_2AlB_4 the two sets of boron $p\sigma$ states are not completely filled, being 0.6 and 0.1 eV above the Fermi level (see Fig. 5). This is a very satisfying outcome, because they still contribute a considerable 0.042 states/(eV spin boron atom) to the DOS at the Fermi level [to be compared to 0.059 and 0.049 states/(eV spin boron atom) in MS2-LiB and C32-MgB_2, respectively[22]]. Because boron orbitals do not overlap across the Li-filled portion of 1010-Li_2AlB_4, the $p\sigma$ states are not dispersed and give rise to the desired, nearly cylindrical two-dimensional Fermi surfaces similar to those of MS-LiB.[12,22,23] In addition, the compound has $p\pi$ Fermi surfaces, as the $p\pi$-bands crossing now happens at about 0.7 eV. The $p\pi$ states DOS of 0.019 states/(eV spin boron atom) is a significant improvement with respect to MS2-LiB, which lacks these states altogether. However, this contribution is still below the value in MgB_2 [0.032 states/(eV spin boron atom)] and, unfortunately, comes at the expense of losing some $p\sigma$ DOS.

Figure 6 shows that boron in 1010-Li_2TiB_4 is too over-doped to have any strong MgB_2-type electron-phonon coupling. The bottom $p\sigma$ band at -1.5 eV is completely filled, and even though the top band is still 0.3 eV above the Fermi

level the steep $\partial E/\partial k$ derivative on the narrow cylinder along Γ-A results in a relatively low DOS of 0.010 states/(eV spin boron atom). 1010-Li_2HfB_4 exhibits similar properties but has a slightly higher $p\sigma$ DOS of 0.017 states/(eV spin boron atom). 1010-Li_2MB_4 compounds with transition metals of valence V and higher present cases of borides with completely filled boron $p\sigma$ states (see Table I).

V. PHONON SOFTENING

As previously discussed,[24] the next step in the analysis of superconducting properties of the proposed materials should be an *ab initio* calculation of the electron-phonon coupling λ. However, the full scale calculations become prohibitively expensive for compounds with large unit cells, and more so if they have nested Fermi surfaces. In the following we attempt to obtain information on the strength of the electron-phonon coupling from the compounds' vibrational properties.

Indeed, it has been previously argued that the unexpected decrease of λ in MS-LiB with respect to that in MgB_2 can be related to the increase in the in-plane boron frequency and to the smaller softening of this mode.[23,24] The considerations were based on the fact that for a zone-center optical phonon mode the softening due to screening by metallic electrons, $\Delta\omega$, is connected to the Fermi-surface average of the square of the electron-phonon matrix element, g, through $\Delta\omega^2 = -4\omega\langle g^2\rangle N(0)$ [$N(0)$ is the electronic DOS at the Fermi level].[23,47,48]

Unfortunately, there is no simple way to evaluate the unscreened frequency in real materials. However, in MgB_2-type superconductors the M-point phonons have wave vectors larger than $2k_F$ and are thus screened much less than the Γ-point phonons. For this reason we will use the $\omega_M - \omega_\Gamma$ difference to reveal how the in-plane boron vibrations soften across a set of binary and ternary layered metal borides. It should be stressed that the above frequency difference cannot be treated as the real softening for quantitative estimates of the electron-phonon coupling; nevertheless, we expect it to be useful for selecting candidates with the strongest electron-phonon coupling.

For the C32-MB_2 diborides and MS2-LiB monoboride, we calculate the frequencies of the in-plane boron mode at Γ and the TO mode at M points in the frozen-phonon approach using the fourth-order corrections and the same settings as described in Refs. 12 and 49. We neglect the anharmonic and nonadiabatic effects since we are interested in general trends. Full phonon spectra in existing metal diborides have been calculated previously,[50,51] and the general inverse dependence of the E_{2g} frequency at Γ on the boron-boron bond length has been pointed out.[51] In Fig. 7 we plot, as functions of the boron-boron bond length a_{B-B}, the Γ- and M-point sets of calculated frequencies. The latter exhibits a much more consistent linear decrease with the bond length for all known metal diborides of groups III-V. One can further discern two subsets (Al, Hf, Zr, Y, and the rest) which have Γ-point frequencies following the linear dependence with similar negative slopes (we see no apparent factor which could be responsible for this behavior). Note that for the electron-rich metal diborides ω_M is below ω_Γ, which illustrates why the

former cannot be considered as the unscreened frequency. However, the calculated values of Γ- and M-point frequencies will be useful as a reference when we examine the vibrational properties of the ternary MS phases derived from the corresponding metal diborides.

As expected, MgB_2 stands out as a compound with a large softening of the frequency at Γ. In addition, Fig. 7 shows that the M-point frequency does not follow the general trend of group-III-V metal diborides either; this behavior cannot be directly related to the electron-phonon coupling with the $p\sigma$ boron states. The phenomenon is explained in Fig. 8 where we plot calculated frequencies for a large set of group-I-II metal diborides. The M-point frequency ω_M for divalent (Be, Mg, and Ca) and monovalent (Li, Cu, Au, Ag, Na, and K) metals shows similar and nearly perfect linear dependences on the boron-boron bond length. One can expect to have the same trends for the unscreened frequency, only it would be shifted up by a constant offset.

These results give a new perspective on the relation between the vibrational properties and the strength of the electron-phonon coupling in LiB discussed in Refs. 23 and 24. As a boride isovalent to MgB_2, LiB follows the $\omega_M(a_{B-B})$ dependence obtained for the Be-Mg-Ca series of diborides shown in Fig. 8. Therefore, one of the key factors in the LiB hardening of the in-plane frequency (with respect to that in MgB_2) is the shortening of the boron-boron bond length, which depends on the metal and the particular filling of the $p\pi$ and $p\sigma$ states of boron. Hence, it follows that the frequency softenings in LiB and MgB_2 are, in fact, comparable.

Finally, we can comment on the superconducting properties of the proposed ternary compounds. The introduction of electron-rich metals (group IV and higher) into 1010-Li_2MB_4 overdopes the boron layers, and causes the vibrational properties to become closer to those of the corresponding diborides: ω_Γ is still above ω_M for Ti and Hf (Fig. 8). 1010-Li_2AlB_4 is a more promising MgB_2-type superconducting material, judging by the pronounced softening of the in-plane boron mode (note that in AlB_2 ω_Γ is harder than ω_M). Unfortunately, aluminum induces the shortening of the bond length and a substantial increase in the in-plane boron frequency, which will likely weaken the electron-phonon coupling[23,24] (Sec. VI is devoted to a more accurate description of this compound). As for the proposed MS phases at other compositions, we find that all ternary systems with negative relative stability for 1010-Li_2MB_4 (Fig. 2) have negative relative stability for 110-Li_4MB_6 as well (the latter are typically 2–7 meV/atom above the line connecting 11-LiB and 1010-Li_2MB_4 and are only metastable). Therefore, if 110-Li_4MB_6 could still be synthesized with large in size transition metals, such as Hf or Ta, the superconducting properties of the boron layer in the "11" portion (which should be well isolated by the double layers of lithium from the electron-rich "0"-unit) would be enhanced due to the stretching of the overall boron bond length in the compound. A similar phenomenon has been recently observed in stretched MgB_2 films.[52] A recent Raman study of the vibrational and superconducting properties of doped MgB_2 has revealed that the adjustment of the frequency alone might not be enough to achieve a higher T_c.[53]

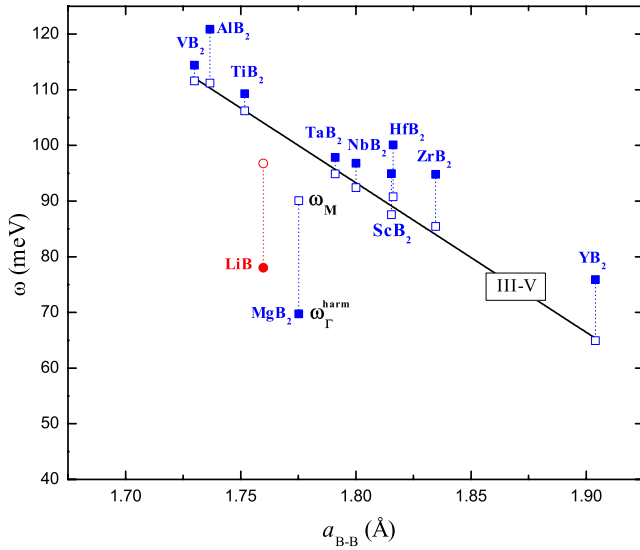The trend shown in Figs. 7 and 8 is corroborated by the well known correlation between the increase in the electron-

FIG. 7. (Color online) Frequency of the in-plane boron phonons at M (open symbols) and Γ (solid symbols) points as a function of boron-boron bond length. The known C32-MB$_2$ diborides are shown as blue squares; the proposed MS2-LiB is shown as red circles. The solid line shows a linear fit of the M-point frequencies for the known diborides with metal valence from III to V.

FIG. 8. (Color online) Frequency of the in-plane boron phonons at M (open symbols) and Γ (solid symbols) for C32-MB$_2$ diborides of group I, II, and III-V metals. The blue squares, black triangles, and red circles correspond to the known, unstable, and proposed (11-LiB and 1010-Li$_2M$B$_4$) compounds, respectively. The linear fits to the sets of M point frequencies are labeled according to the valence of the metal.

phonon coupling and the inevitable dynamical destabilization of the structure[54–58] (a too strong renormalization can cause a Peierls-type distortion, a band Jahn-Teller transformation, or a structural transition[55]). In our considered metal boride prototypes, the specific relation between stability and superconductivity originates from the subtle effects associated with the filling of binding states of boron.

The focus of our study has been the MgB$_2$-type superconductors, while there have been reports on Nb-deficient superconductors based on C32-NbB$_2$ with T_c of nearly 10 K.[5,6] Indeed, it would be interesting to explore the superconducting potential of Li$_2M$B$_4$ compounds (M = V, Nb, and Ta) which would have a non-MgB$_2$-type electron-phonon coupling mechanism.

VI. PHONON SPECTRUM AND ELECTRON-PHONON COUPLING

In the previous sections we have shown that Li$_2$AlB$_4$ has a significant amount of boron $p\sigma$ and $p\pi$ DOS at the Fermi level and exhibits a characteristic softening of the in-plane boron phonon mode at Γ. All these quantities are lower compared to those in MgB$_2$ so that one can expect the superconducting properties of Li$_2$AlB$_4$ to be less appealing. However, a full calculation of the electron-phonon coupling [for all the modes and all **k** points in the Brillouin zone (BZ)] is needed to understand the superconducting properties of Li$_2$AlB$_4$. For example, in MgB$_2$ the intercalant modes are weakly coupled; based on our results for LiB (Ref. 24) the situation could be different in Li$_2$AlB$_4$. In addition, due to symmetry constraints in calculations on periodic systems, energy minimization might not guarantee convergence to an equilibrium free of dynamical instabilities (imaginary phonon frequency
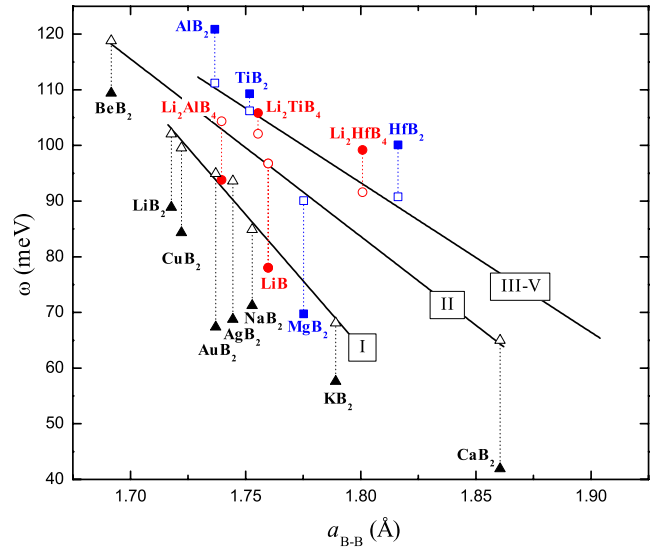
at $\mathbf{q} \neq \Gamma$). Thus, dynamical stability has to be checked by explicit calculation of the phonon frequencies in the whole BZ. In this section we calculate vibrational phonon frequencies and the electron-phonon coupling of Li$_2$AlB$_4$ using density-functional theory in the linear response approach.[59]

We find[60] that the theoretically devised structure of Li$_2$AlB$_4$ is dynamically stable with no imaginary phonon frequencies. The obtained phonon density of states (PHDOS) is plotted in Fig. 9. As it can be seen from the decomposition along selected Cartesian vibrations, B modes are dominant at energies larger than 50 meV. In the low energy region (<50 meV), two clear peaks are seen, one at $\approx$40 meV due to Li vibrations and the other one at 30 meV due to Al vibrations. As expected from the large interlayer spacing between the B layers, B modes are flat in the direction perpendicular to the B layers.

The electron-phonon coupling $\lambda_{\mathbf{q}\nu}$ for a phonon mode ν with momentum $\mathbf{q}$ is

$$\lambda_{\mathbf{q}\nu} = \frac{4}{\omega_{\mathbf{q}\nu}N(0)N_k} \sum_{\mathbf{k},n,m} |g^\nu_{\mathbf{k}n,\mathbf{k}+\mathbf{q}m}|^2 \delta(\epsilon_{\mathbf{k}n})\delta(\epsilon_{\mathbf{k}+\mathbf{q}m}), \quad (2)$$

where the sum is over the Brillouin zone. The matrix element is $g^\nu_{\mathbf{k}n,\mathbf{k}+\mathbf{q}m} = \langle \mathbf{k}n | \delta V / \delta u_{\mathbf{q}\nu} | \mathbf{k}+\mathbf{q}m \rangle / \sqrt{2\omega_{\mathbf{q}\nu}}$, where $u_{\mathbf{q}\nu}$ is the amplitude of the displacement of the phonon, V is the Kohn-Sham potential, and $N(0)$ is the electronic density of states at the Fermi level. The calculated average electron-phonon coupling is $\lambda = \sum_{\mathbf{q}\nu} \lambda_{\mathbf{q}\nu}/N_q \approx 0.41$ (N_k and N_q are the **k**-space and **q**-space mesh dimensions, respectively[60]).
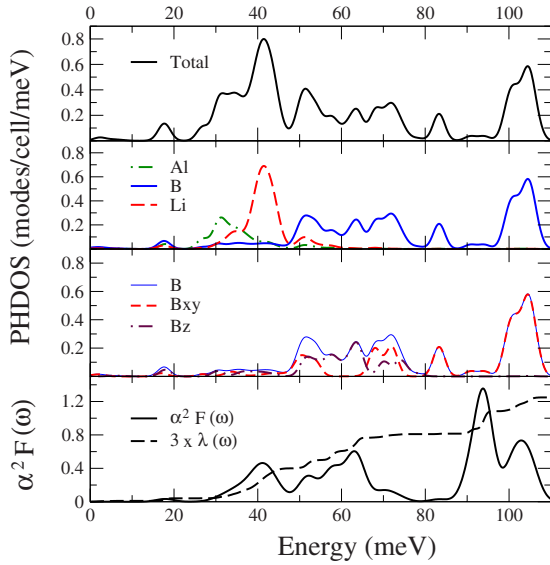
The Eliashberg function

FIG. 9. (Color online) PHDOS decomposed over selected vibrations, Eliashberg function $\alpha^2F(\omega)$ and integrated Eliashberg function $\lambda(\omega)$ in Li$_2$AlB$_4$.

$$\alpha^2F(\omega) = \frac{1}{2N_q}\sum_{\mathbf{q}\nu}\lambda_{\mathbf{q}\nu}\omega_{\mathbf{q}\nu}\delta(\omega-\omega_{\mathbf{q}\nu}) \qquad (3)$$

and the integral $\lambda(\omega) = 2\int_0^\omega d\omega'\,\alpha^2F(\omega')/\omega'$ are shown in Fig. 9. As can be seen, the contribution of the coupling due to in-plane vibration is substantially reduced with respect to MgB$_2$. This confirms what could be qualitatively inferred from the softening calculated in Fig. 8. On the contrary the coupling to intercalant modes is not negligible.

The critical superconducting temperature is estimated using the McMillan formula:[61]

$$T_c = \frac{\langle\omega\rangle_{\log}}{1.2}\exp\left[-\frac{1.04(1+\lambda)}{\lambda-\mu^*(1+0.62\lambda)}\right], \qquad (4)$$

where μ^* is the screened Coulomb pseudopotential and

$$\langle\omega\rangle_{\log} = e^{\frac{2}{\lambda}\int_0^{+\infty}\alpha^2F(\omega)\log(\omega)/\omega d\omega} \qquad (5)$$

the phonon frequencies logarithmic average. We obtain $\langle\omega\rangle_{\log}=59.4$ meV leading to T_c of approximately 3.6 K for $\mu^*=0.1$. This value might be enhanced by multiband effects.

VII. SUMMARY

We have demonstrated that there is a number of Li-M-B systems, in which MS ternary borides gain in stability with respect to MS2-LiB and C32-MB$_2$. The finding suggests that these potential superconductors could be synthesized under normal conditions or grown on metal diboride substrates with a matching lattice constant. We show that some boron states in the MS ternary compounds (derived from those in MS2-LiB and C32-MB$_2$) are still hole-doped and could give rise to the MgB$_2$-type superconductivity. In order to preselect compounds with the strongest electron-phonon coupling we examine the softening of the in-plane boron phonon mode in a large class of metal borides. We find a very well-defined correlation between the frequency of this mode and both the boron-boron bond length and the valence of the metal. This observation allows us to give a new interpretation of the hardening of the in-plane boron phonon mode in MS-LiB and identify one compound, Li$_2$AlB$_4$, that should be a superconductor with T_c of about 3.6 K.

ACKNOWLEDGMENTS

[1] J. Nagamatsu, N. Nakagawa, T. Muranaka, Y. Zenitani, and J. Akimitsu, Nature (London) **410**, 63 (2001).

[2] J. Kortus, O. V. Dolgov, R. K. Kremer, and A. A. Golubov, Phys. Rev. Lett. **94**, 027002 (2005), and references therein.

[3] M. Imai, E. Abe, J. Ye, K. Nishida, T. Kimura, K. Honma, H. Abe, and H. Kitazawa, Phys. Rev. Lett. **87**, 077003 (2001).

[4] H. Rosner, W. E. Pickett, S.-L. Drechsler, A. Handstein, G. Behr, G. Fuchs, K. Nenkov, K.-H. Muller, and H. Eschrig, Phys. Rev. B **64**, 144516 (2001).

[5] A. Yamamoto, C. Takao, T. Masui, M. Izumi, and S. Tajima, Physica C **383**, 197 (2002).

[6] Z.-A. Ren, S. Kuroiwa, Y. Tomita, and J. Akimitsu, Physica C **468**, 411 (2008).

[7] H. Rosner, A. Kitaigorodsky, and W. E. Pickett, Phys. Rev. Lett. **88**, 127001 (2002).

[8] A. M. Fogg, J. B. Claridge, G. R. Darling, and M. J. Rosseinsky,

Chem. Commun. (Cambridge) **12**, 1348 (2003); A. M. Fogg, J. Meldrum, G. R. Darling, J. B. Claridge, and M. J. Rosseinsky, J. Am. Chem. Soc. **128**, 10043 (2006).

[9] T. E. Weller, M. Ellerby, S. S. Saxena, R. P. Smith, and N. T. Skipper, Nat. Phys. **1**, 39 (2005).

[10] N. Emery, C. Herold, M. d'Astuto, V. Garcia, C. Bellin, J. F. Mareche, P. Lagrange, and G. Loupias, Phys. Rev. Lett. **95**, 087003 (2005).

[11] A. Gauzzi, S. Takashima, N. Takeshita, C. Terakura, H. Takagi, N. Emery, C. Hérold, P. Lagrange, and G. Loupias, Phys. Rev. Lett. **98**, 067002 (2007).

[12] A. N. Kolmogorov and S. Curtarolo, Phys. Rev. B **73**, 180501(R) (2006).

[13] P. Zhang, S. Saito, S. G. Louie, and M. L. Cohen, Phys. Rev. B **77**, 052501 (2008).

[14] Inorganic crystal structure database, http://icsd.ill.fr/icsd/index.html

[15] P. Villars, K. Cenzual, J. L. C. Daams, F. Hulliger, T. B. Massalski, H. Okamoto, K. Osaki, A. Prince, and S. Iwata, *Pauling File: Inorganic Materials Database and Design System* (ASM International, Metal Park, OH, 2003).

[16] T. Oguchi, J. Phys. Soc. Jpn. **71**, 1495 (2002).

[17] R. J. Cava, H. W. Zandbergen, and K. Inumaru, Physica C **385**, 8 (2003).

[18] F. Bernardini and S. Massidda, Europhys. Lett. **76**, 491 (2006).

[19] F. Bernardini and S. Massidda, Phys. Rev. B **74**, 014513 (2006).

[20] A. V. Palnichenko, O. M. Vyaselev, and N. S. Sidorov, JETP Lett. **86**, 272 (2007).

[21] R. V. Chepulskii, I. I. Mazin, and S. Curtarolo, First-principles search for potential high temperature superconductors in the Mg-B-*A* (*A*=alkali and alkaline earth metals) system with high boron content, 2008.

[22] A. N. Kolmogorov and S. Curtarolo, Phys. Rev. B **74**, 224507 (2006).

[23] A. Y. Liu and I. I. Mazin, Phys. Rev. B **75**, 064510 (2007).

[24] M. Calandra, A. N. Kolmogorov, and S. Curtarolo, Phys. Rev. B **75**, 144506 (2007).

[25] A. N. Kolmogorov, R. Drautz, and D. G. Pettifor, Phys. Rev. B **76**, 184102 (2007).

[26] J. Q. Li, L. Li, F. M. Liu, C. Dong, J. Y. Xiang, and Z. X. Zhao, Phys. Rev. B **65**, 132505 (2002).

[27] S. Curtarolo, D. Morgan, K. Persson, J. Rodgers, and G. Ceder, Phys. Rev. Lett. **91**, 135503 (2003).

[28] D. Morgan, G. Ceder, and S. Curtarolo, Meas. Sci. Technol. **16**, 296 (2005).

[29] S. Curtarolo, D. Morgan, and G. Ceder, CALPHAD: Comput. Coupling Phase Diagrams Thermochem. **29**, 163 (2005).

[30] P. E. Blochl, Phys. Rev. B **50**, 17953 (1994).

[31] J. P. Perdew, K. Burke, and M. Ernzerhof, Phys. Rev. Lett. **77**, 3865 (1996).

[32] G. Kresse and J. Hafner, Phys. Rev. B **47**, 558 (1993).

[33] G. Kresse and J. Furthmuller, Phys. Rev. B **54**, 11169 (1996).

[34] G. Kresse and D. Joubert, Phys. Rev. B **59**, 1758 (1999).

[35] H. J. Monkhorst and J. D. Pack, Phys. Rev. B **13**, 5188 (1976); **16**, 1748 (1977).

[36] Figure 3 of Ref 22.

[37] Figure 2 of Ref 22.

[38] M. Sluiter, D. de Fontaine, X. Q. Guo, R. Podloucky, and A. J. Freeman, Phys. Rev. B **42**, 10460 (1990).

[39] M. H. F. Sluiter, Y. Watanabe, D. de Fontaine, and Y. Kawazoe, Phys. Rev. B **53**, 6137 (1996).

[40] T. Ito and I. Higashi, Acta Crystallogr., Sect. B: Struct. Sci. **39**, 239 (1983).

[41] T. Sun, Y. G. Zhao, R. Fan, X. P. Zhang, B. G. Liu, Y. H. Xiong, and P. J. Li, J. Supercond. **17**, 473 (2004).

[42] Consideration of these binary Li-B and Al-B compounds with large unit cells and fractional occupancies of atomic sites is beyond the scope of the present study.

[43] M. Monni, C. Ferdeghini, M. Putti, P. Manfrinetti, A. Palenzona, M. Affronte, P. Postorino, M. Lavagnini, A. Sacchetti, D. Di Castro, F. Sacchetti, C. Petrillo, and A. Orecchini, Phys. Rev. B **73**, 214508 (2006).

[44] F. E. Wang, M. A. Mitchell, R. A. Sutula, and J. R. Holden, J. Less-Common Met. **61**, 237 (1978).

[45] M. Wörle, R. Nesper, G. Mair, and H. G. von Schnering, Solid State Sci. **9**, 459 (2007), and references therein.

[46] K. Togano, P. Badica, Y. Nakamori, S. Orimo, H. Takeya, and K. Hirata, Phys. Rev. Lett. **93**, 247004 (2004).

[47] I. I. Mazin and V. P. Antropov, Physica C **385**, 49 (2003).

[48] C. O. Rodriguez, A. I. Liechtenstein, I. I. Mazin, O. Jepsen, O. K. Andersen, and M. Methfessel, Phys. Rev. B **42**, 2692 (1990).

[49] K. Kunc, I. Loa, K. Syassen, R. K. Kremer, and K. Ahn, J. Phys.: Condens. Matter **13**, 9945 (2001).

[50] K.-P. Bohnen, R. Heid, and B. Renker, Phys. Rev. Lett. **86**, 5771 (2001).

[51] R. Heid, B. Renker, H. Schober, P. Adelmann, D. Ernst, and K.-P. Bohnen, Phys. Rev. B **67**, 180510(R) (2003).

[52] A. V. Pogrebnyakov, J. M. Redwing, S. Raghavan, V. Vaithyanathan, D. G. Schlom, S. Y. Xu, Qi Li, D. A. Tenne, A. Soukiassian, X. X. Xi, M. D. Johannes, D. Kasinathan, W. E. Pickett, J. S. Wu, and J. C. H. Spence, Phys. Rev. Lett. **93**, 147006 (2004).

[53] W. X. Li, Y. Li, R. H. Chen, R. Zeng, S. X. Dou, M. Y. Zhu, and H. M. Jin, Phys. Rev. B **77**, 094517 (2008).

[54] L. R. Testardi, in *Physical Acoustics*, edited by W. P. Mason and R. N. Thurston (Academic, New York, 1973).

[55] W. E. Pickett, Physica C **468**, 126 (2008).

[56] F. Cordero, R. Cantelli, G. Giunchi, and S. Ceresara, Phys. Rev. B **64**, 132503 (2001).

[57] S. Zherlitsyn, B. Lüthi, V. Gusakov, B. Wolf, F. Ritter, D. Wichert, S. Barilo, S. Shiryaev, C. Escribe-Filippini, and J. L. Tholence, Eur. Phys. J. B **16**, 59 (2000).

[58] M. Braden, W. Reichardt, E. Elkaim, J. P. Lauriat, S. Shiryaev, and S. N. Barilo, Phys. Rev. B **62**, 6708 (2000).

[59] S. Baroni, S. de Gironcoli, A. Dal Corso, and P. Giannozzi, Rev. Mod. Phys. **73**, 515 (2001).

[60] We use the QUANTUM-ESPRESSO code (www.pwscf.org), norm-conserving pseudopotentials, the generalized gradient approximation (PBE) and a 60 Rydberg cutoff for the kinetic energy. We perform the electronic integration using $8 \times 8 \times 8$ **k**-point mesh. The dynamical matrices were computed on a $N_q = 4 \times 4 \times 4$ **q**-point mesh centered at Γ. The electron-phonon coupling was computed using a $N_k = 30 \times 30 \times 30$ **k**-point mesh.

[61] W. L. McMillan, Phys. Rev. **167**, 331 (1968).